# *The Effect of Intrinsic and Acquired Resistances on Chemotherapy Effectiveness*

**Silvia A. Menchón**

**Acta Biotheoretica**
Mathematical and philosophical foundations of biological and biomedical science

ISSN 0001-5342
Volume 63
Number 2

Acta Biotheor (2015) 63:113-127
DOI 10.1007/s10441-015-9248-x

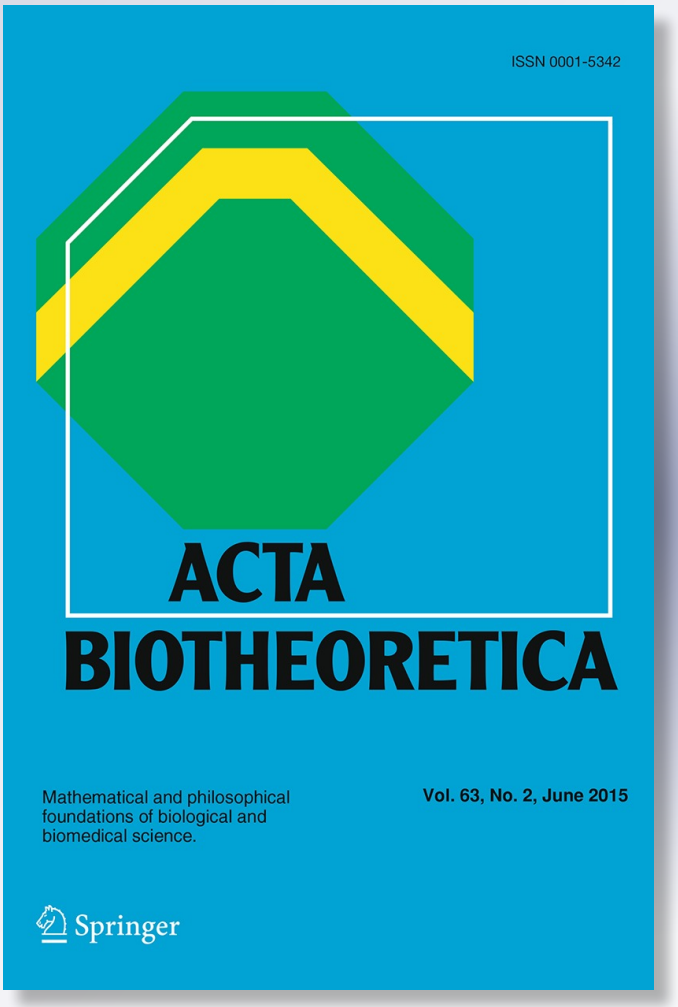


Springer

Acta Biotheor (2015) 63:113–127
DOI 10.1007/s10441-015-9248-x

REGULAR ARTICLE

# The Effect of Intrinsic and Acquired Resistances on Chemotherapy Effectiveness

**Silvia A. Menchón**

Received: 27 December 2013 / Accepted: 20 February 2015 / Published online: 8 March 2015


**Abstract** Although chemotherapy is one of the most common treatments for cancer, it can be only partially successful. Drug resistance is the main cause of the failure of chemotherapy. In this work, we present a mathematical model to study the impact of both intrinsic (preexisting) and acquired (induced by the drugs) resistances on chemotherapy effectiveness. Our simulations show that intrinsic resistance could be as dangerous as acquired resistance. In particular, our simulations suggest that tumors composed by even a small fraction of intrinsically resistant cells may lead to an unsuccessful therapy very quickly. Our results emphasize the importance of monitoring both intrinsic and acquired resistances during treatment in order to succeed and the importance of doing more experimental and genetic research in order to develop a pretreatment clinical test to avoid intrinsic resistance.

**Keywords** Mathematical modeling and simulations · Chemotherapy · Intrinsic resistance · Acquired resistance

## 1 Introduction

When mutations are present in oncogenes and/or tumor suppresor genes, uncontrolled cell division occurs, leading to cancer (Priestman 2008). Although chemotherapy has been used for many years and is one of the most common treatments for cancer, it has been only partially successful (DeVita 1983; DeVita et al. 2008; McKinnell et al. 2006). Resistance to the drugs is the most common cause of failure. It is known that the antitumor action of chemotherapeutic drugs can be abolished by many different mechanisms. If these mechanisms are preexisting,

S. A. Menchón (✉)
IFEG-CONICET and FaMAF, Universidad Nacional de Córdoba, Medina Allende s/n, Ciudad Universitaria, 5000 Córdoba, Argentina
e-mail: menchon@famaf.unc.edu.ar

i.e., if they are present before the drug application, the resistance is called *intrinsic resistance*. On the other hand, if those mechanisms are induced by the action of the drug, i.e., cancer cells develop resistance during the treatment, it is named *acquired resistance* (Johnstone et al. 2002). A proper understanding of both intrinsic and acquired resistances is very important. Clinical studies suggest that nearly 50 % of cancer patients suffer from tumors that are intrinsically resistant to chemotherapy (Lippert et al. 2008), and cellular models have shown that the ability to acquire resistance may also be present during the early stage of tumor progression (Raguz and Yagüe 2008). Although there are many clinical procedures to evaluate and monitor acquired resistance, there is almost no pretreatment clinical test to evaluate the presence of intrinsically resistant cells.

Various mathematical models have been developed to describe and study drug resistance (Goldie and Coldman 2009). The nature of the applied methods depends on the biological question they address. We find deterministic and stochastic as well as discrete (agent-based) and continuum (differential equations) models. As examples of the different approaches we can mention: logistic growth and Lotka Volterra competition (Kansal et al. 2000), models where the rate at which cells become resistant depends on the drug dose (Coldman and Goldie 1985), pulsed chemotherapy considering that the drug affects cells instantaneously (Panetta 1998), a mathematical model for the simultaneous application of chemotherapy and immunotherapy (de Pillis et al. 2009), regrowth of tumor cords (Bertuzzi et al. 2003), partial differential equations considering different drug kinetics (Norris et al. 2006), optimization techniques (Murray and Coldman 2003), birth and death processes (Foo and Michor 2010) and reaction-diffusion approaches (Garner et al. 2005; Lecca and Morpurgo 2012), among others. Although single-drug resistance is considered in most of these works, mathematical models addressing multidrug resistance have also been developed (Lavi et al. 2012). Additionally, we refer the interested reader to the following papers: d'Onofrio and Gandolfi (2010), Frieboes et al. (2009), Swierniak et al. (2009) and Silva and Gatenby (2010). Most of the models focus on the temporal evolution of different cell populations, and just a few study the spatial distribution of solid heterogeneous tumors. Some recent examples of spatio-temporal models are: a cellular automaton model (Jackson 2003), a stochastic reaction-diffusion model of non-small-cell lung cancer growth (Lecca and Morpurgo 2012) and our previous work (Menchón and Condat 2011).

In this article, we extend and modify the model used previously (Menchón and Condat 2008, 2009, 2011) to incorporate intrinsic and acquired resistances. This model is based on the fact that competition for nutrients and space is a crucial growth-controlling factor, and it pays close attention to the local spatial distributions of nutrients and cells. Opposite to general models, we do not consider a very simplified symmetric scenario; growth depends on the local resources availability. Our goal here is to study how resistance could affect an otherwise successful therapy; we are interested in evaluating and comparing the tumor aggressiveness and its evolution concerning intrinsic and acquired resistances.

In our previous work (Menchón and Condat 2011), we showed that those cells that were quiescent at the moment when the drug was applied could be resistant and later become proliferative depending on the local microenvironment and nutrient

availability (we will refer to these cells as "quiescent resistant cells" in the conclusions section). In that approach, the drug affected cell reproduction and induced cell apoptosis. Thus, once the active outer shield had been depleted by the drug action, larger amounts of the nutrient could reach mostly quiescent interior cells, which eventually became proliferative again and then sensitive to the drug. However, if the delay was long enough, the level of drug concentration could be too low to be effective. Thus, cells that were quiescent at the moment when the drug was applied become "naturally" resistant. As was shown in that work, the resistance of quiescent cells is enough to induce tumor relapse.

In this work, we focus on intrinsic and acquired resistances, and we want to evaluate how a successful treatment can fail because of them. In order to analyze just the effect of intrinsic or acquired resistance, we would like to suppress any other kind of resistance, i.e., for instance, we would like to avoid the effect of quiescent cell resistance. In other words, we want to create a theoretical scenario near reality, which allows us to determine whether only the presence of intrinsic or acquired resistant cells is enough to induce relapse and how it would be for each type of resistance. Since in the presence of intrinsic or acquired resistance, the active outer shield is not fully depleted, and all the nutrients that reach the interior cells have to be distributed between the resistant cells (which can proliferate) and sensitive cells. The possible relapse due to quiescent cells should be much less than the one reported in Menchón and Condat (2011); then, the effect of the drug concentration level on the sensitive cells (which was explained above) can be neglected. We will also assume that the effect of the drug on the cancer cells is fast compared with the temporal evolution of the tumor. Therefore, we consider that the drug has an instantaneous effect upon application. We do not model either the drug delivery or its spatial distribution; instead, we assume that the drug immediately affects all sensitive cells. Due to the drug action, sensitive cells stop their cell cycle and become nonproliferative. After the drug is applied, resistant cells will appear with some probability. A more detailed description of the model is given in the next section.

Using realistic parameter values, we show that intrinsic resistance can be as aggressive as acquired resistance. Both intrinsic and acquired resistances can induce tumor relapse with even a small fraction of resistant cancer cells. In particular, a tumor composed of 2 % (or more) of intrinsic resistant cells may lead to an unsuccessful treatment. Our simulations emphasize the importance of diagnosing intrinsic resistance before treatment starts.

## 2 The Model

Here we extend the basic growth model developed by Scalerandi et al. (1999) to describe cancer growth. In this model, the tissue is represented by a network whose node points are associated with a volume element that contains many cells and nutrient molecules. In order to model intrinsic and acquired resistances, we will add a few rules and consider that most of the cancer cells become nonproliferating because of the drug action. Since our goal is to describe the evolution of a tumor

that is composed by sensitive and nonsensitive cancer cells, we write down the equations of a generalized model considering the presence of $N$ kinds of cancer cells. In this work $N = 2$.

### 2.1 Growth Rules

Healthy, cancerous and dead cells coexist at each node point, their concentrations being denoted by $h(\mathbf{i})$, $c^l(\mathbf{i})$ and $d^l(\mathbf{i})$, respectively, where $l = 1, 2, \ldots, N$. For simplicity, we consider a single critical nutrient that diffuses through the tissue, with diffusion coefficient $\alpha'$. It is called the free nutrient, and its concentration at the $\mathbf{i}$-th node is denoted by $p(\mathbf{i}, t)$. The total cell concentration is considered to be uniform and normalized, i.e., $h(\mathbf{i}) + \sum_{l=1}^{N} \left(c^l(\mathbf{i}) + d^l(\mathbf{i})\right) = 1$. The free nutrient is absorbed by the healthy cells at a rate $\gamma_0$.

The rules governing cancer growth are the following:

G1. *Feeding*. The free nutrient is absorbed by cancer cells and converted into a bound nutrient. The absorption rate is proportional to $p(\mathbf{i})$ at low free nutrient concentrations, and it saturates to a constant value, $\gamma_{as}^l$, at high concentrations. We model the absorption rate by

$$\gamma^l(\mathbf{i}) = \gamma_{as}^l \left(1 - e^{-p(\mathbf{i})}\right).$$

G2. *Consumption*. The bound nutrient is consumed by $\mathbf{i}$-th node cells at the rate

$$\beta^l(\mathbf{i}) = \beta_{as}^l \left(1 - e^{-q^l(\mathbf{i})/c^l(\mathbf{i})}\right),$$

where $q^l(\mathbf{i})$ is the bound nutrient (by $l$-type cancer cells) concentration, and the denominator $c^l(\mathbf{i})$ has been included in the exponent because each cell can consume only its own bound nutrient.

G3. *Death*. If the average amount of the bound nutrient per cell, $q^l(\mathbf{i})/c^l(\mathbf{i})$, is below a given threshold $Q_D^l$, a fraction $r_D^l c^l(\mathbf{i})$ of cancer cells dies, where $r_D^l$ is a constant.

G4. *Mitosis*. If the average amount of bound nutrient per cell is above a given threshold $Q_M^l$ ($Q_M^l > Q_D^l$), a fraction $f^l(\mathbf{i})$ of healthy cells is transformed into cancer cells. This fraction is given by

$$f^l(\mathbf{i}) = h(\mathbf{i}) + \left(r_M^l c^l(\mathbf{i}) - h(\mathbf{i})\right) \Theta\left(h(\mathbf{i}) - r_M^l c^l(\mathbf{i})\right),$$

where $\Theta$ is Heaviside's step function and $r_M^l$ is a constant.

G5. *Migration*. If the average amount of free nutrient per cell, $p(\mathbf{i}) / \sum_{l=1}^{N} c^l(\mathbf{i})$, is below a migration threshold, $P_D^l$, cells of type $l$ at the $\mathbf{i}$-th node migrate to its neighboring nodes. Since healthy cells are less mobile and aggressive than cancer cells, we assume that they are eliminated when cancer cells arrive in such a way that the total cell concentration is preserved.

## 2.2 Implementation

We represent the tissue of interest by a two-dimensional square grid, with lattice constant $\ell$ and node points $\mathbf{i} = (\ell i; \ell j)$. The nutrient is supplied by a single capillary vessel situated at the lower edge of the lattice. The nutrient concentration in the blood vessel is constant, $p((\ell i; 0), t) = P_0$. Periodic boundary conditions are used for the left and right boundaries. Thus, for a tissue composed by healthy cells and $N$ kinds of cancer cells, the free nutrient evolution is given by:

$$\begin{aligned} p(\mathbf{i}, t+\tau) = p(\mathbf{i}, t) + \tau \Bigg( & \sum_{\mathbf{i}'} \frac{\alpha'}{\ell^2} (p(\mathbf{i}', t) - p(\mathbf{i}, t)) \\ & - \gamma_0 p(\mathbf{i}, t) h(\mathbf{i}, t) - \sum_{l=1}^{N} \gamma^l c^l(\mathbf{i}, t) \Bigg), \end{aligned} \tag{1}$$

where $\tau$ is the discrete temporal step. The first term in the bracket has the contribution due to diffusion between nearest neighbors; the second and third terms represent the consumption due to healthy and cancer cells, respectively. According to rules G3 and G4, cancer cell populations are updated by:

$$\begin{aligned} c^l(\mathbf{i}, t) \longrightarrow c^l(\mathbf{i}, t) - r_D^l c^l(\mathbf{i}, t) \Theta\left[Q_D^l c^l(\mathbf{i}, t) - q^l(\mathbf{i}, t)\right] \\ + f^l(\mathbf{i}, t) \Theta\left[q^l(\mathbf{i}, t) - c^l(\mathbf{i}, t) Q_M^l\right]. \end{aligned} \tag{2}$$

The second and third terms on the right-hand side represent the variations due to death and mitosis, respectively. The corresponding equation for the dead cell population is given by:

$$d^l(\mathbf{i}, t) \longrightarrow d^l(\mathbf{i}, t) + r_D^l c^l(\mathbf{i}, t) \Theta\left[Q_D^l c^l(\mathbf{i}, t) - q^l(\mathbf{i}, t)\right]. \tag{3}$$

The cancer cell population can also be modified because of migration. The equation representing rule G5 is given by:

$$\begin{aligned} c^l(\mathbf{i}, t+\tau) = c^l(\mathbf{i}, t) + \frac{\tau}{\ell^2} \Bigg\{ & h(\mathbf{i}, t) \sum_{\mathbf{i}'} \alpha_1^l(\mathbf{i}', t) c^l(\mathbf{i}', t) \\ & - \alpha_1^l(\mathbf{i}, t) c(\mathbf{i}, t) \sum_{\mathbf{i}'} h(\mathbf{i}', t) \Bigg\}, \end{aligned} \tag{4}$$

where $\alpha_1^l(\mathbf{i}, t) = \alpha^l \Theta[p(\mathbf{i}, t) - \sum_{l=1}^{N} c^l(\mathbf{i}, t) P_D^l]$ as well as $\alpha^l$ is the diffusion coefficient for the $l$-type cancer cells. Since the dead cells do not migrate, there is no need to change their concentration because of migration. Each time cancer cell populations are modified by rules G3-G5, the healthy cell population has to be updated by $h(\mathbf{i}, t) \longrightarrow 1 - \sum_{l=1}^{N} (c^l(\mathbf{i}, t) + d^l(\mathbf{i}, t))$. The bound nutrient concentrations are updated according to rules G1, G2 and G5, since cancer cells migrate carrying their bound nutrient. All these contributions are represented by the following equation:

$$q^l(\mathbf{i}, t+\tau) = q^l(\mathbf{i}, t) + \tau\Big\{\gamma^l(\mathbf{i}, t)c^l(\mathbf{i}, t) - \beta^l(\mathbf{i}, t)c^l(\mathbf{i}, t) + \frac{h(\mathbf{i}, t)}{\ell^2}\sum_{\mathbf{i}'}\alpha_1^l(\mathbf{i}', t)q^l(\mathbf{i}', t) - \frac{\alpha_1^l(\mathbf{i}, t)}{\ell^2}q^l(\mathbf{i}, t)\sum_{\mathbf{i}'}h(\mathbf{i}', t)\Big\}. \tag{5}$$

The first term in brackets represents the absorption of free nutrient, the second term contains the consumption, and the last terms represent the migration between nearest neighbors.

## 2.3 Resistance

Since in this work we are interested in the effect of intrinsic and acquired resistances, we consider that the drug is fully effective against sensitive cancer cells and has an instantaneous effect upon application. In other words, we assume that at time $t_c$ the drug is applied and immediately affects all sensitive cells. The drug effect is to stop the cell cycle, i.e., all the sensitive cells become nonproliferative after $t_c$. From this moment, sensitive cancer cells cannot reproduce anymore because of the action of the drug, and only resistant cells can reproduce. Sensitive cells do not die from the action of the drug, they just stop their cell cycle and cannot reproduce, but they still consume nutrients, occupy space and migrate. Thus, we consider that the resistant cells differ from the sensitive cells in having their cell cycle active. We add a few rules according to the nature of the resistance.

### *2.3.1 Intrinsic Resistance*

We consider that a cell is intrinsically resistant if it has inherent resistance to chemotherapeutic drugs, i.e., its resistance is independent of the presence of the drug. We consider that just a fraction of the tumor cells can be intrinsically resistant, and we take a constructive approach to generating the distribution of those cells at the moment when therapy is applied. To model cancer growth with intrinsically resistant cells, we add the following rules:

I1. For $t < t_c$, at each time the rule G4 is implemented, we choose a random number $v$, uniformly distributed between 0 and 1. If $v < \phi$ all the cells in node $\mathbf{i}$ become resistant. The parameter $\phi$ is thus the probability to become resistant. This procedure ensures that older cells have a bigger chance of becoming resistant.

I2. At $t = t_c$ cells that are not resistant are defined as sensitive and stop their cell cycle. Mitosis is not allowed for them anymore.

### *2.3.2 Acquired Resistance*

The acquired resistance is drug-induced, i.e., cells become resistant because of the interaction with the drug. The new rules for this type of resistance are:

A1. At $t = t_c$ all the cells become sensitive, and rule G4 ceases to be operative.
A2. For $t \geq t_c$, at each time we should check the mitosis threshold, we choose a random number $v$, uniformly between 0 and 1. If $v < \phi$ all the cells inside node $\mathbf{i}$ become resistant, and rule G4 starts to be operative for them again.

The conversion from sensitive to resistant cells can be expressed by the following equations:

$$
\begin{aligned}
c^1(\mathbf{i}, n\Delta t) &\rightarrow c^1(\mathbf{i}, n\Delta t)(1 - \Theta(\phi - v)),\\
c^2(\mathbf{i}, n\Delta t) &\rightarrow c^1(\mathbf{i}, n\Delta t)\Theta(\phi - v),\\
q^1(\mathbf{i}, n\Delta t) &\rightarrow q^1(\mathbf{i}, n\Delta t)(1 - \Theta(\phi - v)),\\
q^2(\mathbf{i}, n\Delta t) &\rightarrow q^1(\mathbf{i}, n\Delta t)\Theta(\phi - v),
\end{aligned}
$$

where $c^1(\mathbf{i}, t)$ and $c^2(\mathbf{i}, t)$ represent the sensitive and resistant cell population, respectively. Here $q^1(\mathbf{i}, t)$ and $q^2(\mathbf{i}, t)$ are the concentrations of bound nutrient for each cell population. This conversion can only take place at integer multiples of $\Delta t = 12$ h, the time at which the rule G4 is going to be implemented (I1) or should have been implemented (A2). In the case of intrinsic resistance, these equation are considered if $n\Delta t < t_c$; for acquired resistance, they are implemented if $n\Delta t > t_c$. In both cases for $t > t_c$, rule G4 ceases to be operative for $c^1(\mathbf{i}, t)$, but it is implemented for $c^2(\mathbf{i}, t)$. In other words, intrinsically resistant cells are generated randomly before drug application, and acquired resistant cells are generated randomly after therapy has started. For all time, type 2 cancer cells are proliferative.

## 3 Results

Initially, we consider a healthy tissue with stationary nutrient distribution. At $t = 0$, a cancer seed of type 1 is placed at the center of the lattice, and a tumor starts growing at the center of a completely healthy tissue. Tumor evolution is governed by rules G1–G5 and simulated as in our previous works (Menchón and Condat 2008, 2009, 2011). We use the value of the parameters shown in Table 1. A

**Table 1** Numerical values of computational parameters

| Symbol | Unit | Value | References |
|---|---|---|---|
| $\ell$ | μm | 33 | |
| $\tau$ | h | 0.001 | |
| $P_0$ | Mm | 5.5 | Fang et al. (2004) |
| $\alpha'$ | $cm^2/h$ | 0.001 | Casciari et al. (1988); Jiang et al. (2005) |
| $\gamma$ | 1/h | 0.002 | Drasdo and Höhme (2005); Jiang et al. (2005) |
| $\gamma_{as}$ | 1/h | 200 | Drasdo and Höhme (2005); Freyer and Sutherland (1985) |
| $\beta_{as}$ | 1/h | 5 | Kole et al. (1999) |
| $\alpha$ | $cm^2/h$ | $8.3 \times 10^{-8}$ | Chaplain and Matzavinos (2006); Swanson et al. (2003) |

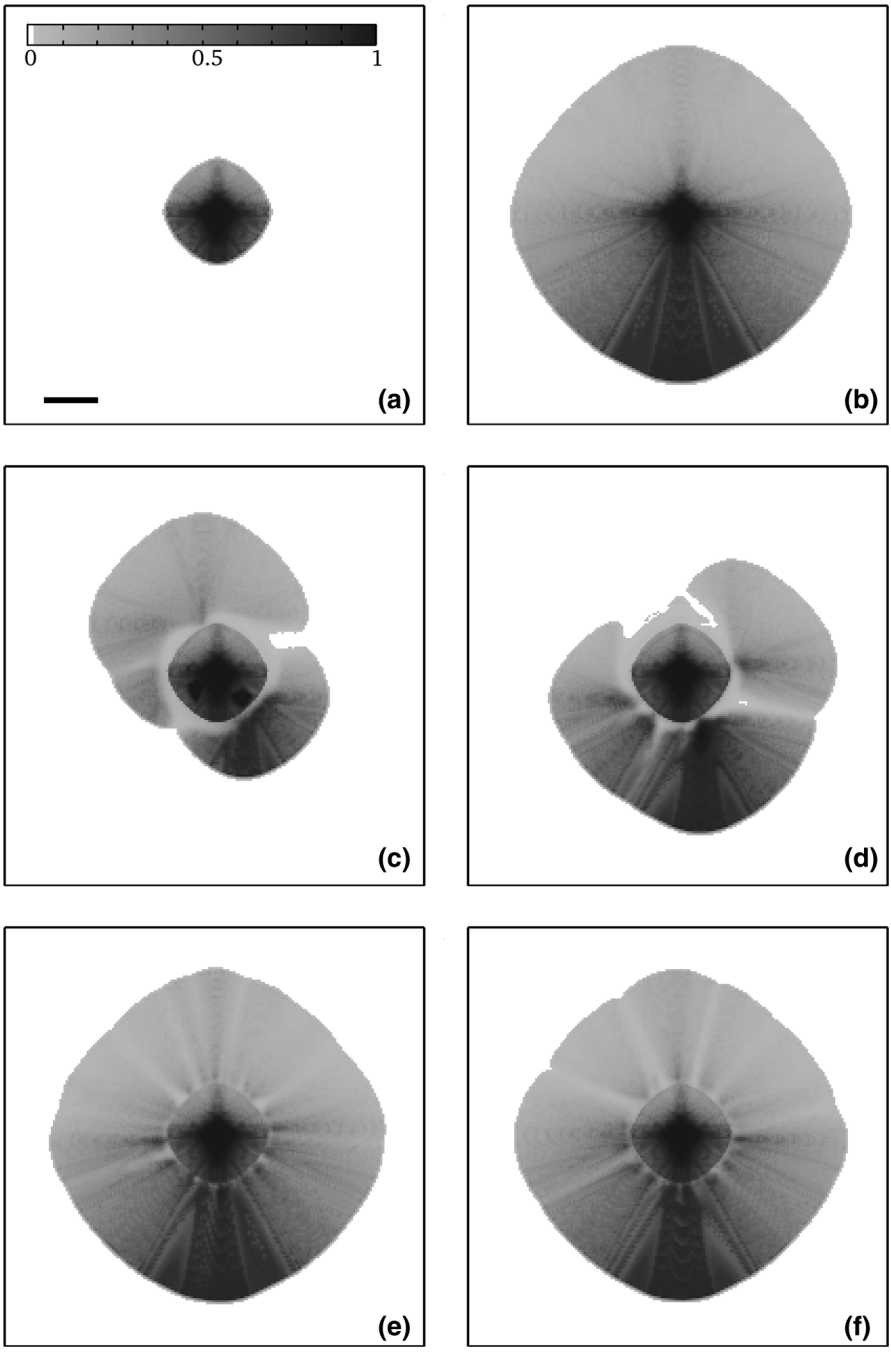

◀**Fig. 1** Snapshots of growing tumors: 30 days after seeding (**a**); 150 days after seeding (**b**); 120 days of treatment, tumor with intrinsic resistance $\phi = 0.0005$ (**c**); 120 days of treatment, tumor with acquired resistance $\phi = 0.0005$ (**d**); 120 days of treatment, tumor with intrinsic resistance $\phi = 0.1$ (**e**); 120 days of treatment, tumor with acquired resistance $\phi = 0.1$ (**f**). *Scale bar* 1 mm. For these simulations, parameters shown in Table 1 are used

complete explanation of the parameters related to cell growth is given in Menchón and Condat (2008).

We assume that at time $t_c$, a drug is applied. Due to the effect of the therapy, sensitive cells stop their cell cycle immediately. For $t \geq t_c$, the tumor will be formed by two populations: one sensitive, i.e., nonproliferative (1) and the other resistant, which is able to proliferate (2). If the therapy were not applied, cancer cells at the tumor boundary would proliferate faster than the inner cells because of the difference in space and nutrient availability between those regions. However, if the therapy is applied, all sensitive cells stop replicating. Thus, free nutrient consumption, for a tumor with sensitive cells, is reduced in comparison with a tumor without sensitive cells because there are fewer cells absorbing it. After a few days, the nutrient availability in the tumor interior increases (due to diffusion), and resistant cells in those regions can proliferate if they have space availability. In other words, once therapy has been applied, the absorption rate of the free nutrient at the tumor periphery falls and increased amounts of nutrient reach the tumor interior, allowing resistant cell proliferation. If $\phi$ is small, ($\phi \approx 5 \times 10^{-4}$), most of the cells that are intrinsically resistant are located in the tumor interior. This means that they probably need to wait longer until nutrient availability increases locally to be able to proliferate, a process that may be even slower because of the lack of space. Therefore, the cancer cells may first need to migrate and find their way to the boundary before the tumor starts growing again. However, it occurs more frequently that cells with acquired resistance are located near the tumor boundary. Thus, at the moment they become resistant, it is likely that they have nutrient and space availability. According to our simulations, if $\phi$ is high enough, ($\phi \approx 0.1$), around 35 % of live cells are intrinsically resistant at the moment when therapy is applied. Although the tumor reduces its growth rate when therapy begins, in a short time resistant cells can reactivate growth, leading to a tumor similar to the one that would have resulted without any therapy. In Fig. 1a, we show a snapshot of a growing tumor at the moment when the therapy is applied. In panel (c), we show a simulation of tumor evolution after 120 days of therapy considering only intrinsic resistance and $\phi = 0.0005$. In panel (d), we also show a simulation of tumor evolution after 120 days of therapy with $\phi = 0.0005$, but now this simulation presents only acquired resistance. Spots of higher cell concentration can be seen in the interior of the original tumor in panel (c), showing that some intrinsically resistant cells were initially located in the inner region. Once resistant cells arrive at the boundary, i.e., a place with enough nutrient and space availability, regrowth takes place, generating regions that are composed mostly by resistant cells and giving to the tumor a clustering structure. Although the simulation in panel (d) represents a more aggressive tumor than the simulation in panel (c), it is important to notice that the tumor simulated in panel (c) is composed by a small fraction of intrinsically

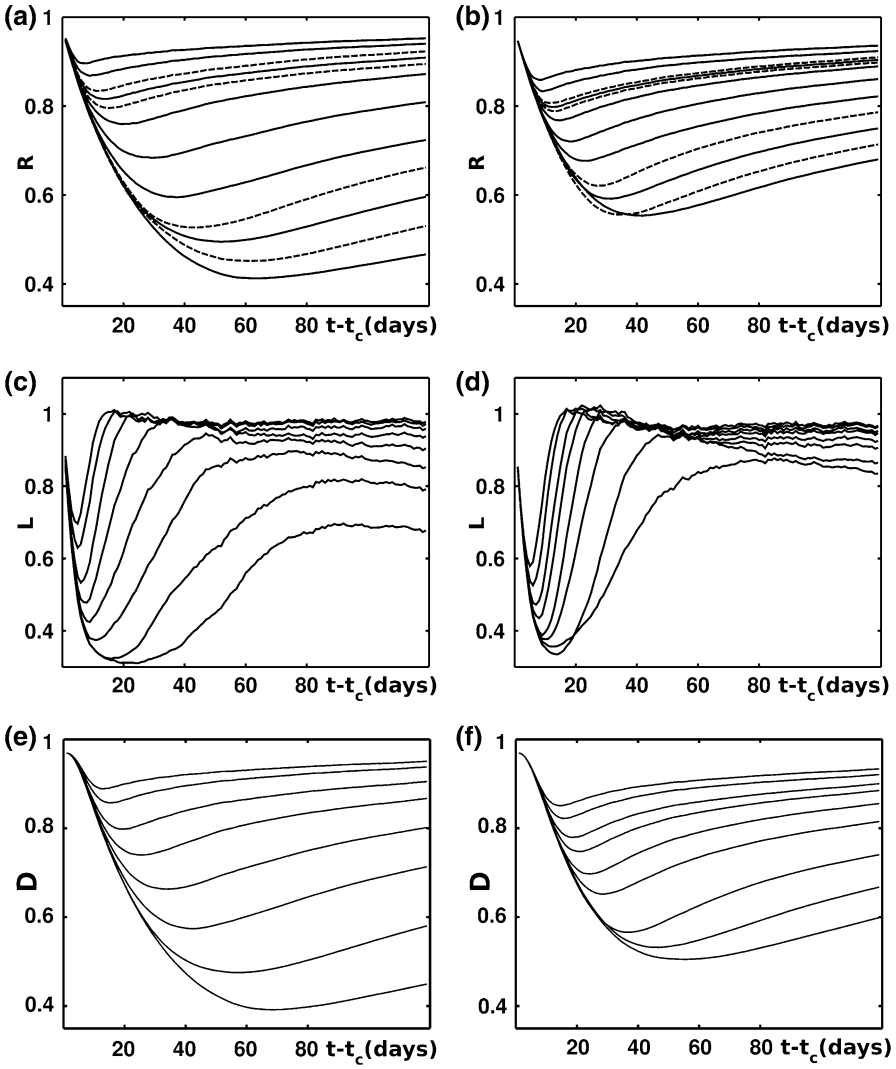


**Fig. 2** Ratio between the total number of tumor cells with and without therapy, $R(t)$, for intrinsic (**a**) and acquired (**b**) resistances as a function of time (*solid lines*, average of seven runs). For a more clear figure only standard deviations for selected *curves* are plotted (*dashed lines*). Ratio between the total number of live tumor cells with and without therapy, $L(t)$, for intrinsic (**c**) and acquired (**d**) resistances as a function of time (*solid lines*, average of seven runs). Ratio between the total number of dead tumor cells with and without therapy, $D(t)$, for intrinsic (**e**) and acquired (**f**) resistances as a function of time (*solid lines*, average of seven runs). For all the panels and from the *top down* $\phi = 0.1$, $\phi = 5 \times 10^{-2}$, $\phi = 2 \times 10^{-2}$, $\phi = 10^{-2}$, $\phi = 5 \times 10^{-3}$, $\phi = 2 \times 10^{-3}$, $\phi = 10^{-3}$, $\phi = 5 \times 10^{-4}$

resistant cells; less than 1 % of live cancer cells are resistant at the moment when therapy is applied. In panels (e) and (f), we show simulations after 120 days of therapy with intrinsic and acquired resistances, respectively. For both, we have used $\phi = 0.1$. In panel (b), we show tumor evolution in the absence of therapy.

Simulations in panels (e) and (f) represent tumors that seem to be equally aggressive as that represented by the simulation shown in panel (b).

A measure of the apparent success of a therapy is given by the time evolution of the ratio $R(t)$ of the total number of (live and dead) cancer cells in a tumor subject to therapy to the total number of cancer cells in the same tumor in the absence of therapy. A successful therapy will keep $R(t) \ll 1$ for a long time. For a single application of therapy, we expect $R(t)$ to undergo a sharp decrease and then to slowly grow toward unity as the tumor regrows. We also expect $R(t)$ to be a monotonically increasing function of the resistance degree. Indeed, this can be seen in Fig. 2a, b, where we show $R(t)$ for the cases of intrinsic and acquired resistances, respectively, and for different values of $\phi$. The solid lines represent the average over seven runs, and the dashed lines are the standard deviation for selected curves. It is clear that for $\phi \approx 0.1$, in both cases the total number of cancer cells is very similar to that for a tumor without any therapy. However, they are not identical, $R$ being greater for intrinsic resistance. Now, for small $\phi$ we can observe a considerable reduction in the number of total cancer cells. This reduction is even stronger for intrinsic resistance having a reduction of about 50 % for $\phi = 0.0005$ after 120 days of therapy. However, for the same $\phi$ we just have a reduction of $\approx$30% after 120 days of therapy with acquired resistance.

If we instead study the ratio $L(t)$ between the total numbers of *live* cancer cells (see Fig. 2c, d), we can also observe that for a small $\phi$ the tumor with acquired resistance is more aggressive than that with intrinsic resistance, a situation that is reversed for greater $\phi$. Analyzing the ratio $L(t)$, we observe an important reduction a few days after therapy has been applied. This reduction is followed by a fast increase due to repopulation. This fast growth can generate tumors with more live cancer cells than their counterparts without therapy (see Fig. 2d at $t - t_c \approx$20 days for high $\phi$). Growth slows down in the following days because of the increase in the number of cancer cells, which enhances the local competition for limited resources. Again, for small (high) $\phi$ values, tumors with acquired (intrinsic) resistance have a faster repopulation than those with intrinsic (acquired) resistance. The ratio $D(t)$ between the total numbers of *dead* cancer cells (see Fig. 2e, f) is very similar to $R(t)$ due to the fact that the live cells are a small fraction of the tumor (in general located at the outer rim).

The fraction of resistant cells at the moment when therapy is applied, in the simulations performed with intrinsic resistance and $\phi = 2 \times 10^{-3}$, is less than 2 %. These results indicate that the therapy effectiveness can be really affected even with a very small fraction of resistant cells, since for these simulations $R = 0.72$ and $L = 0.85$. Figure 3 shows the ratio $R$ as a function of the percentage of intrinsically resistant cells at the moment when therapy is applied for different times. Tumors composed by a very low percentage of intrinsically resistant cells, around 0.1 %, can be considered as tumors that still respond to the therapy. However, a fast relapse takes place in tumors with 2 % or more of intrinsically resistant cells at the moment when treatment starts.

In Stein et al.'s paper (2008), clinical data for several patients with prostate cancer are reported. Many of the curves presented in that work correspond to acquired resistance. Unfortunately, in the present work we do not model the drug-

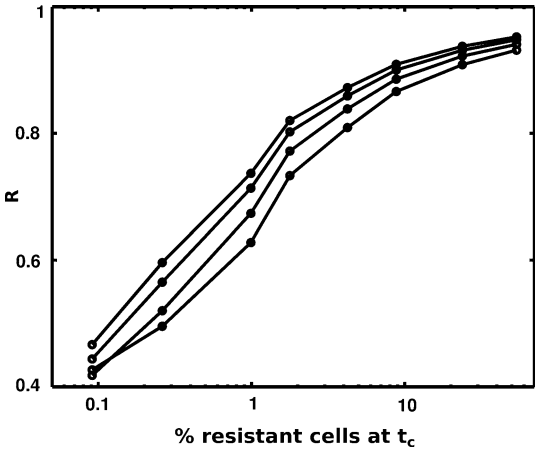


**Fig. 3** Ratio between the total number of tumor cells with and without therapy, $R$, for intrinsic resistance as a function of the percentage of intrinsic resistant cells at the moment when therapy is applied. Each *curve* represents a different time. From *top down*: $t - t_c = 120$ days, $t - t_c = 100$ days, $t - t_c = 75$ days, $t - t_c = 50$ days

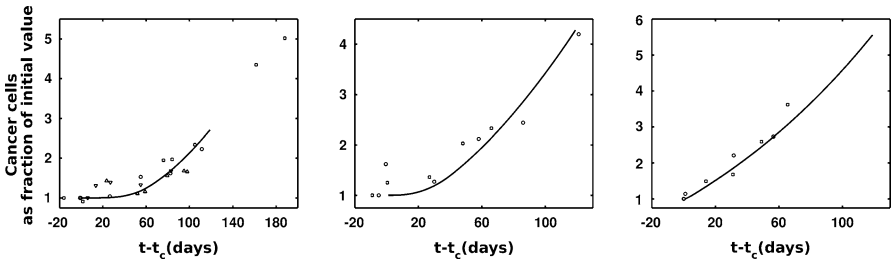


**Fig. 4** Comparison between clinical data of the prostate-specific antigen level as a fraction of the value at the start of treatment (*dots*) and simulations of intrinsic resistance (*solid lines*). In the *left panel* $\phi = 0.0005$, in the *middle panel* $\phi = 0.002$ and in the *right panel* $\phi = 0.1$. The clinical data were reported in the supplementary material of Stein et al. (2008) and correspond to patients 13 (*downward triangles*), 42 (*circles*), 73 (*upward triangles*) and 67 (*squares*) in the *left panel*; 57 (*circles*) and 63 (*squares*) in the *middle panel*; 18 (*squares*) and 97 (*circles*) in the *right panel*

cell interaction, and then we cannot model the temporal window between the drug application and presence of resistant cells for each patient. However, some of the clinical data are related to intrinsic resistance since they present almost no improvement after the drug has been applied. In Fig. 4, we compare some clinical data reported in the supplementary information of Stein et al. (2008) with our simulations of intrinsic resistance. In this figure, the total number of cancer cells is shown as a fraction of the value at the start of treatment versus time in days. The agreement between our simulations and the clinical data indicates the great importance of diagnosing intrinsic resistance before treatment starts.

## 4 Conclusions

Cytotoxic agents are effective against tumor cells because they reproduce faster than normal cells. However, since cells of vital organs also grow quickly, they may also be destroyed or damaged, causing severe side effects. Therefore, ineffective

chemotherapy treatments make patients suffer from both tumor growth and side effects of the drugs. It is known that nearly 50 % of cancer patients have tumors that are formed by intrinsic chemotherapy-resistant cells (Lippert et al. 2008). Although there are some commercial tests that register tumor resistances with an accuracy of around 90 %, there are no standard clinical procedures to identify intrinsic resistance (Lippert et al. 2008). On the other hand, nowadays it is possible to monitor drug resistance during treatment by positron-emission tomography (PET), which allows determining the metabolic activity of neoplastic tissue (Lippert et al. 2011). Intrinsic resistance tests and PET could be useful for the early detection of acquired resistance and give an idea of the time interval from drug administration to resistance development. Although these techniques to detect individual resistance are available, they can be very expensive and out of reach for most patients.

In this article, we used a simple spatio-temporal mathematical model to describe intrinsic and acquired resistances. Using realistic values and a minimum number of rather general assumptions, we have shown how an otherwise successful therapy can fail because of the presence of resistant cells. We have considered that resistant cells only differ from sensitive cancer cells in having an active cell cycle. In the case of intrinsic resistance, we have seen that simulations of tumors with just about 1 % of their live cancer cells being resistant may affect treatment effectiveness (Fig. 1c), and those with 35 % of their live cancer cells being resistant lead to the complete failure of the treatment (Fig. 1e). Although before treatment intrinsically resistant cells are randomly distributed and well mixed with sensitive cells, after drug application, they find their way out to regions with more resources, as a result leading to tumors with clustering structures of sensitive and resistant cells. This clustering of structures has also been observed in kidney (Gerlinger et al. 2012) and breast cancer considering phenotype clustering (Almendro et al. 2014). Our simulations also show that, for tumors with acquired resistance, it takes only a few days (between 5 and 10) to have tumor regrowth after the first resistant cell appears (Fig. 2d). This aggressiveness is similar to that for tumors composed of a small fraction of intrinsically resistant cells at the moment when therapy is applied. According to our model, the delay in tumor relapse for intrinsic resistance is basically caused by the time resistant cells need in order to migrate to regions with more space and nutrients. The agreement in the comparison between our results and clinical data seems to validate our assumptions.

The model presented here has some limitations. In particular, we do not consider the effect of the drug and pressure in the extracellular matrix. We also do not consider drug distribution and quiescent cell resistance. Although these effects deserve to be considered in the future, chemotherapy effectiveness would be even more reduced if we added them to the model. In particular, if drug administration and distribution dynamics are included, according to Menchón and Condat (2011) and considering that the drug is distributed by diffusion, the nutrient concentration inside the tumor increases after the drug has been applied, allowing the interior cells to live longer. This result suggests that, in general, an intrinsically resistant cell population would survive, even if the drug does not have an instantaneous effect. However, it might have a different impact on the tumor evolution, since interior intrinsically resistant cells should compete for space and nutrients with “quiescent

resistant cells" (see introduction). In this case, it would be interesting to evaluate whether therapy effectiveness is mainly reduced because of "quiescent resistant cells" or because of intrinsically resistant cells. Thus, in a future work, it would be worth analyzing the tumor composition and its temporal evolution, studying the ratio of "quiescent resistant cells" to intrinsically resistant cells in the function, for instance, of the drug distribution speed. Even more, the fact of including drug distribution would allow considering different schedules for drug application and the possibility to use optimal control theory tools, like in Swan (1990), to evaluate different clinical procedures and determine the best strategy for each patient.

We have shown that tumors with resistance may repopulate very quicly even in cases with a small probability of developing resistant cells. Our results underline the crucial importance of an early diagnosis of resistance and the need to intensify the development of individual resistance tests in order to provide more effective treatments.

**Acknowledgments** This work was partially supported by SeCyT-UNC (project 3072011-0100436) and CONICET (PIP 112-200801-00772) (Argentina). I would like to express my gratitude to Prof. Carlos Condat for his guidance, helpful advice and inspiring discussions.

## References

Almendro V, Cheng YK, Randles A, Itzkovitz S, Marusyk A, Ametller E, Gonzalez-Farre X, Munoz M, Russnes HG, Helland A, Rye IH, Borresen-Dale AL, Maruyama R, van Oudenaarden A, Dowsett M, Jones RL, Reis-Filho J, Gascon P, Gonen M, Michor F, Polyak K (2014) Inference of tumor evolution during chemotherapy by computational modeling and in situ analysis of genetic and phenotypic cellular diversity. Cell Rep 6:514–527

Bertuzzi A, d'Onofrio A, Fasano A, Gandolfi A (2003) Regression and regrowth of tumour cords following single-dose anticancer treatment. Bull Math Biol 65:903–931

Casciari JJ, Sotirchos SV, Sutherland RM (1988) Glucose diffusivity in multicellular tumor spheroids. Cancer Res 48:3905–3909

Chaplain M, Matzavinos A (2006) Mathematical modeling of spatio-temporal phenomena in tumor immunology. In: Friedman A (ed) Tutorials in mathematical biosciences III: cell cycle, proliferation, and cancer. Springer, New York, pp 131–183

Coldman AJ, Goldie JH (1985) Role of mathematical modeling in protocol formulation in cancer chemotherapy. Cancer Treat Rep 69:1041–1048

de Pillis L, Fister KR, Gu W, Collins C, Daub M, Gross D, Moore J, Preskill B (2009) Mathematical model creation for cancer chemo-immunotherapy. Comput Math Methods Med 10:165–184

DeVita VT (1983) Progress in cancer management. Keynote address. Cancer 51:2401–2409

DeVita VT, Lawrence TS, Rosenberg SA, DePinho RA, Weinberg RA (2008) DeVita, Hellman, and Rosenberg's cancer: principles and practice of oncology. Lippincott Williams & Wilkins, Philadelphia, USA

d'Onofrio A, Gandolfi A (2010) Resistance to antitumor chemotherapy due to bounded-noise-induced transitions. Phys Rev E 82(061):901

Drasdo D, Höhme S (2005) A single-cell-based model of tumor growth in vitro: monolayers and spheroids. Phys Biol 2:133–147

Fang J, Sullivan M, McCutchan TF (2004) The effects of glucose concentration on the reciprocal regulation of rRNA promoters in plasmodium falciparum. J Biol Chem 279:720–725

Foo J, Michor F (2010) Evolution of resistance to anti-cancer therapy during general dosing schedules. J Theor Biol 263:179–188

Freyer JP, Sutherland RM (1985) A reduction in the in situ rates of oxygen and glucose consumption of cells in EMT6/Ro spheroids during growth. J Cell Physiol 124:516–524

Frieboes HB, Edgerton ME, Fruehauf JP, Rose FRAJ, Worrall LK, Gatenby RA, Ferrari M, Cristini V (2009) Prediction of drug response in breast cancer using integrative experimental/computational modeling. Cancer Res 69:4484–4492

Garner AL, Lau YY, Jackson TL, Uhler MD, Jordan DW, Gilgenbach RM (2005) Incorporating spatial dependence into a multicellular tumor spheroid growth model. J Appl Phys 98:1–8

Gerlinger M, Rowan AJ, Horswell S, Larkin J, Endesfelder D, Gronroos E, Martinez P, Matthews N, Stewart A, Tarpey P, Varela I, Phillimore B, Begum S, McDonald NQ, Butler A, Jones D, Raine K, Latimer C, Santos CR, Nohadani M, Eklund AC, Spencer-Dene B, Clark G, Pickering L, Stamp G, Gore M, Szallasi Z, Downward J, Futreal PA, Swanton C (2012) Intratumor heterogeneity and branched evolution revealed by multiregion sequencing. New Engl J Med 366:883–892

Goldie JH, Coldman AJ (2009) Drug resistance in cancer: models and mechanisms. Cambridge University Press, Cambridge, UK

Jackson TL (2003) Intracellular accumulation and mechanism of action of doxorubicin in a spatio-temporal tumor model. J Theor Biol 220:201–213

Jiang Y, Pjesivac-Grbovic J, Cantrell C, Freyer JP (2005) A multiscale model for avascular tumor growth. Biophys J 89:3884–3894

Johnstone RW, Ruefli AA, Lowe SW (2002) Apoptosis: a link between cancer genetics and chemotherapy. Cell 108:153–164

Kansal AR, Torquato S, Chiocca EA, Deisboeck TS (2000) Emergence of a subpopulation in a computational model of tumor growth. J Teor Biol 207:431–441

Kole AC, Plaat BEC, Hoekstra HJ, Vaalburg W, Molenaar WM (1999) FDG and L-[1-11C]-tyrosine imaging of soft-tissue tumors before and after therapy. J Nucl Med 40:381–386

Lavi O, Gottesman MM, Levy D (2012) The dynamics of drug resistance: a mathematical perspective. Drug Resist Update 15:90–97

Lecca P, Morpurgo D (2012) Modelling non-homogeneous stochastic reaction–diffusion systems: the case study of gemcitabine-treated non-small cell lung cancer growth. BMC Bioinform. doi:10.1186/1471-2105-13-S14-S14

Lippert TH, Ruoff HJ, Volm M (2008) Resistance in malignant tumors: Can resistance assays optimize cytostatic chemotherapy? Pharmacology 81:196–203

Lippert TH, Ruoff H, Volm M (2011) Current status of methods to assess cancer drug resistance. Int J Med Sci 8:245–253

McKinnell RG, Parchment RE, Perantoni AO, Pierce GB, Damjanov I (2006) The biological basis of cancer. Cambridge University Press, New York, USA

Menchón SA, Condat CA (2008) Cancer growth: predictions of a realistic model. Phys Rev E 78:022901

Menchón SA, Condat CA (2009) Modeling tumor cell shedding. Eur Biophys J 38:479–485

Menchón SA, Condat CA (2011) Quiescent cells: a natural way to resist chemotherapy. Phys A 390:3354–3361

Murray JM, Coldman AJ (2003) The effect of heterogeneity on optimal regimens in cancer chemotherapy. Math Biosci 185:73–87

Norris ES, King JR, Byrne HM (2006) Modelling the response of spatially structured tumours to chemotherapy: drug kinetics. Math Comput Model 43:820–837

Panetta JC (1998) A mathematical model of drug resistance: heterogeneous tumors. Math Biosci 147:41–61

Priestman T (2008) Cancer chemotherapy in clinical practice. Springer-Verlag, London

Raguz S, Yagüe E (2008) Resistance to chemotherapy: new treatments and novel insights into an old problem. Br J Cancer 99:387–391

Scalerandi M, Romano A, Pescarmona GP, Delsanto PP, Condat CA (1999) Nutrient competition as a determinant for cancer growth. Phys Rev E 59(2):2206–2217

Silva AS, Gatenby RA (2010) A theoretical quantitative model for evolution of cancer chemotherapy resistance. Biol Direct 5:25

Stein WD, Figg WD, Dahut W, Stein AD, Hoshen MB, Price D, Bates SE, Fojo T (2008) Tumor growth rates derived from data for patients in a clinical trial correlate strongly with patient survival: a novel strategy for evaluation of clinical trial data. Oncologist 13:1046–1054

Swan GW (1990) Role of optimal control theory in cancer chemotherapy. Math Biosci 101:237–284

Swanson KR, Bridge C, Murray JD, Alvord EC (2003) Virtual and real brain tumors: using mathematical modeling to quantify glioma growth and invasion. J Neurol Sci 216(1):1–10

Swierniak A, Kimmel M, Smieja J (2009) Mathematical modeling as a tool for planning anticancer therapy. Eur J Pharmacol 625:108–121